COBEM 2021 26th International Congress of Mechanical Engineering
ABCM Associação Brasileira de Engenharia e Ciências Mecânicas
November 22-26, 2021, Virtual Congress, Brazil

COB-2021-0759
COMPARISONS BETWEEN TWO TRANSIENT SIMULATION APPROACHES APPLIED TO A DUAL-EVAPORATOR REFRIGERATOR

Guilherme Z. Santos
Christian J. L. Hermes
POLO Laboratories, Mechanical Engineering Department, Federal University of Santa Catarina, Florianópolis, SC, Brazil
guizsantos@polo.ufsc.br

Abstract. *The present work focuses on the comparison between two distinct strategies for modeling the transient behavior of a household refrigerator: quasi-steady-state and fully transient. Both modeling strategies were employed to simulate the behavior of a refrigerator with two evaporators arranged in parallel (one for the fresh-food, the other for the freezer and ice maker). In addition to the two evaporators with forced convection, the system is comprised of an oil-free linear compressor, a forced air condenser, a 3-way valve upstream of two capillary tubes – one for the freezer and another for the fresh-food – and a check valve at freezer evaporator outlet. For the capillary tube, an artificial neural network was trained using results from a first-principles model. A semi-empirical model was developed for the linear compressor, where the capacity control is achieved by varying the piston displacement. In the case of the fully transient, first-principles models were proposed following a moving boundaries scheme for the evaporators and finite volumes for the condenser. In the case of the quasi-steady-state approach, the refrigerant loop was modeled in steady-state considering prescribed evaporator superheating and condenser subcooling. The closing parameters of the mathematical models, such as overall thermal conductance and heat capacity of the refrigerated compartments, performance curves of the heat exchangers, air flow rates in the refrigerated compartments were determined experimentally using a climatized chamber as well as wind tunnel facilities. The models were implemented in Modelica language, which allows for the temporal solution of the differential and algebraic equations system through the DASSL ODE solver. The model estimates were compared with each other and with experimental counterparts. With regard the experiments, the fully transient model proved to be more accurate, particularly during the pull-down regime, presenting, however, some numerical instabilities. On the other hand, the quasi-steady-state approach proved to be as accurate as fully the transient during the cycling regime, but much more robust. In comparison to the experimental data, an RMS error of 5% was observed for energy consumption and 2°C for temperatures in both cases. Regarding the simulation speed, the quasi-steady-state method, which was capable of simulating about ~13 min/s$_{CPU}$, was approximately 6 times faster than the fully transient model.*

Keywords: *household refrigerator, numerical transient simulations, multiple evaporators, linear compressor, Modelica*

1. INTRODUCTION

In modern days, refrigerators are an essential appliance in any home. In Brazil, the most recent Survey of Possessions and Habits of Use, carried out by Eletrobrás in 2005, disclosed that 96% of electrified households had at least one refrigerator (Procel, 2005). Additionally, the same survey concluded that 99% of refrigerators operate on a permanent basis, *i.e.*, they are never turned off. From this point of view, it is expected that this type of appliance has a significant part in the national energy consumption. In fact, the survey indicated that refrigerators and freezers together account for the largest share of the final consumption of electricity in Brazilian homes, ~27% (Procel, 2005).

As a way of helping the diligent consumer and aiming at promoting the efficient use of electricity, many countries have started labeling policies that grade household appliances from most to less efficient. This energy rating is taken by the domestic refrigerator industry as a competitive factor. Additionally, there is a tendency for the grading system to become more and more strict. Therefore, an investigation of opportunities to improve energy efficiency in domestic refrigerators is justified.

In the Brazilian market, the best-selling domestic refrigerator is the combined type, *i.e.*, separated fresh- and frozen-food compartments. As combined refrigerators make up for 84% of the models listed by INMETRO (INMETRO, 2021), this paper is focused on this type of appliance. In general, refrigeration systems have their performance characterized by the coefficient of performance (COP), defined as the ratio between refrigeration capacity ($\dot{Q}_e$) produced in the evaporator and electrical power ($\dot{W}$) consumed by the system. For combined refrigerators, two COPs can be calculated, one for the freezer and another for the cooler. For an ambient temperature of 32°C, and taking the reference temperatures of -18°C for the former and 5°C for the latter, the Carnot's COP are 5.1 and 10.3, respectively, these being the maximum admissible values for the COP of each refrigerated compartment at the given reference

temperatures. Therefore, at the aforementioned temperature levels, the maximum COP of a combined refrigerator is between 5 and 10.

However, among the existing refrigerator models, some makes use of only one evaporator, responsible for cooling both compartments simultaneously. Thus, ideally, the evaporating temperature is close to that of the freezer, so the COP of this sort of combi refrigerator is at most 5. At this point, there is an opportunity for significant improvement for combined refrigerators, that is, design a cycle architecture with dedicated evaporators for each compartment. In fact, there are already dual-evaporator refrigerator models in the Brazilian market. However, the way the evaporators are structured in the refrigeration circuit can considerably influence the performance gains.

Figure 1 illustrates some of the architectures that employ two evaporators under study at the moment, obtained from a search in the open literature. The cycles proposed in Figures 1a and 1b are similar in their way of operation, as they both work in two modes: freezer only or both evaporators. The major difference between the two lies in the use of the ejector, which has been discussed in recent decades and its purpose in the refrigeration cycle is, in essence, to recover the energy wasted due to isenthalpic expansion in the capillary tube (Radermacher and Kim, 1996; Butrymowicz *et al.*, 2014). In Figure 1c, the operation of both evaporators simultaneously does not occur, as the compressor works either in the freezer or in the cooler. The major advantage of this cycle is to operate at higher evaporating temperatures during operation in the fresh-food.

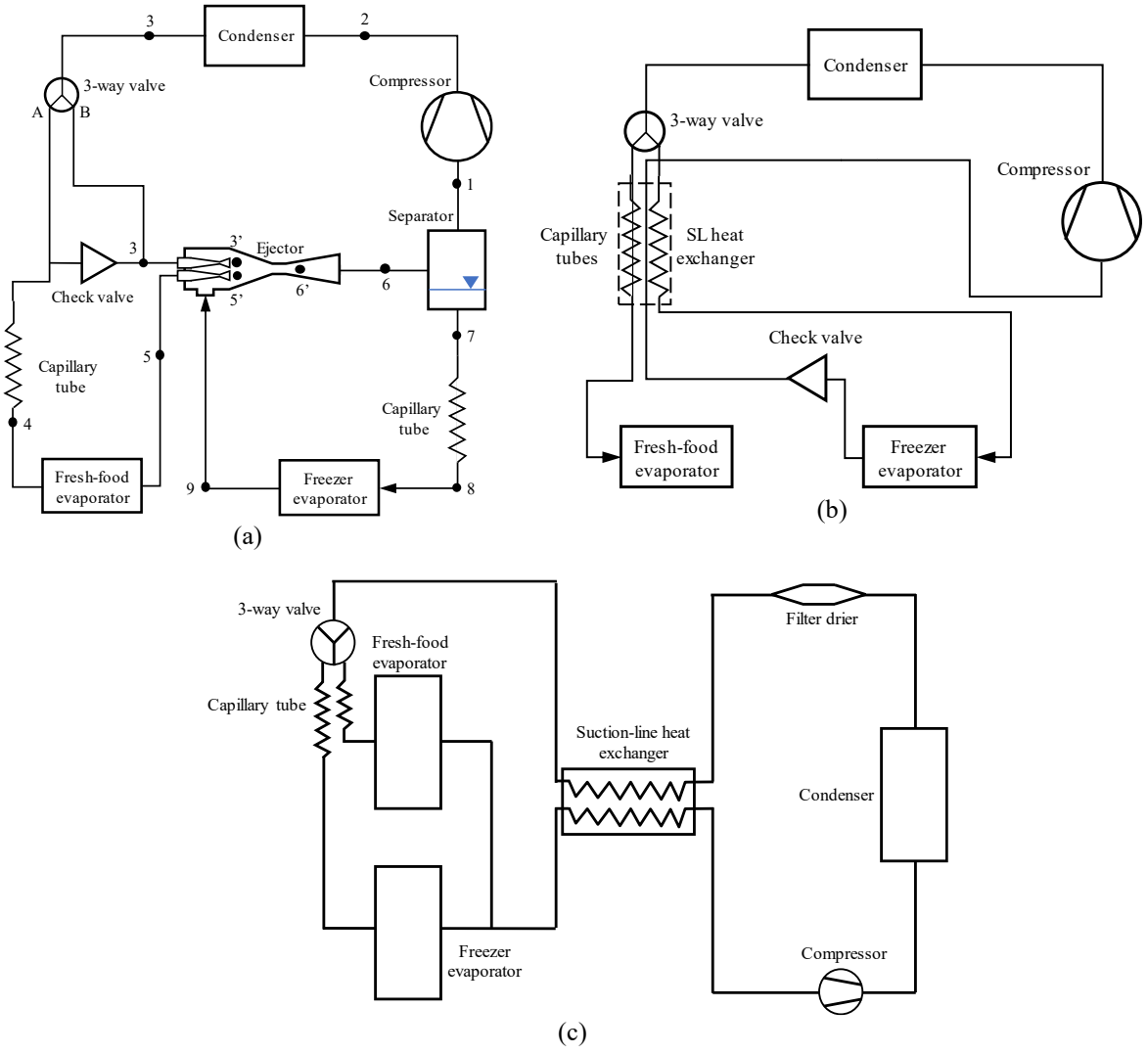

Figure 1. Cycle architectures in recent studies
Adapted from (a) Zhou *et al.* (2013), (b) Yoon *et al.* (2011), and (c) Lu and Ding (2006)

Aside from improving the refrigerator cycle architecture, the manufacturer may also choose to improve the refrigerator efficiency by employing more efficient components, or also by using more sophisticated control logics with variable expansion devices (Knabben, 2019). However, making changes to the refrigerator and evaluating, experimentally, its performance is a highly onerous task - particularly for companies that develop several models of refrigerators simultaneously - the use of computational tools for this purpose has been advocated in the literature

(Negrão and Hermes, 2011). There are several methods for simulating a refrigerator. In essence, it is possible to select the quasi-steady-state approach, which neglects the transients associated with the refrigerant migration in the refrigeration loop, or the fully transient model, which is based on evolutionary equations for the temperatures, pressures and enthalpies of the refrigerant. In both cases, the temperature transients associated with the refrigerated compartments are also accounted for.

Jakobsen (1995) has carried out significantly detailed work regarding the simulation and optimization of domestic refrigerators. In his work, three mathematical models were put forward: a fully transient, a quasi-steady-state and a steady-state model. The numerical implementations of the quasi-steady-state and fully transient models were performed in Pascal language. Although the results obtained by Jakobsen have shown good agreement with the experiments, the global model adopted for the exchangers is not sufficient to properly capture the degree of superheating and subcooling in the evaporator and condenser outputs, respectively.

Shah *et al.* (2003) also performed transient simulations in closed cycles, adopting moving boundary models for heat exchangers, which allows for obtaining a spatial distribution of properties in the exchanger at a low computational cost. On the other hand, it is necessary to consider all possible states of the exchanger, which implies in discontinuities and a large number of constraints in the implementation. The model was coded in Matlab and, despite presenting a sophisticated development of mathematical models, was focused on the control of the refrigeration system for air conditioning applications.

Hermes (2000) developed transient models for the components of the refrigeration cycle of domestic appliances and validated them against experimental data. In this case, the models developed for heat exchangers followed a finite volume scheme, where it is possible to capture the spatial distributions of properties inside the heat exchanger (temperature, enthalpy, vapor quality, etc.). Later, Hermes (2006) proposed more sophisticated component models and performed the coupling them, formulating an explicit transient model for the closed-loop refrigeration system. The implementation was done in Fortran, taking advantage of the notorious high performance of this language.

Borges *et al.* (2011) used the quasi-steady-state modeling strategy to simulate a combined cooler which employed a single evaporator with fan and damper. The model is based on assuming degrees of superheating and subcooling in the evaporator and condenser outputs, respectively (Jakobsen, 1995; Hermes *et al.*, 2009). The model developed by Borges *et al.* (2011) was programmed in EES (Klein, 2011). In a later work, Borges (2013) introduced a sub-model for the capillary tube, thus it was no longer necessary to prescribe superheating at the evaporator outlet. In addition, Borges (2013) also implemented a moving-boundary model for the evaporator, eliminating the need to assume that the compressor mass flow rate is equal to that of the capillary tube. In this way, the evaporator transient was captured by the model. Finally, Borges (2013) simulated events such as door openings and frost formation on the evaporator, evaluating the impact of these phenomena on the performance of the refrigerator.

Diniz *et al.* (2019) carried out a work focusing on the compressor, aiming at evaluating its performance in detail during the on-off operation of the refrigerator. For that, they used a quasi-steady-state model for the refrigeration system where transients were determined by energy balances in the heat exchangers and in the refrigerated cabinet. In comparison with the experimental data, the compressor model presented a good prediction of the indicator diagram, with deviations of 1% for the power consumption and 3% for the mass flow rate. After validation, the model was used to investigate possible improvements in the compressor considering the refrigeration system COP.

As it can be noted, previous studies were developed in a variety of programming languages/platforms: Pascal (Jakobsen, 1995), Fortran (Hermes, 2000, 2006), Matlab (Shah *et al.*, 2003) and EES (Borges, 2013), which are structured programming languages, except for EES, which is equation-based, although none of them is focused on solving dynamic problems. The Modelica language, employed by Diniz *et al.* (2019), is an object-oriented, equation-based language that is focused on the solution of dynamic problems. It has gained strength in the scientific community over the past decade, however lacking mathematical models for the refrigeration sector. In light of what was exposed, the present study aims to make use of the Modelica language, implementing both a fully transient model as well as a quasi-steady-state algorithm in order to evaluate and compare these modeling strategies for a dual-evaporator refrigeration system.

2. BASELINE REFRIGERATION SYSTEM

The present study has taken as reference a French-door Bottom-mount (FDBM) refrigerator (as shown in Figure 2), which was assembled with a parallel dual-evaporator cycle architecture. The refrigeration loop has a spiral finned forced-draft condenser, two fin-on-tube forced-draft evaporators, a linear oil-free variable-capacity compressor, a 3-way valve, two capillary tubes with internal heat exchangers, a check valve, and a heat loop. Aside from the fresh- and frozen-food compartments, the refrigerator has an additional ice making compartment which is located at the fresh-food door and cooled down with air diverted from the freezer by means of a dedicated fan.

Extensive experimental work was performed in order to fully characterize the refrigerator. Using both hydraulic and thermohydraulic wind tunnels it was possible to determine the air flow rate (V) through the freezer, ice maker and fresh-food compartments, as well as gather the heat exchanger and fan performance curves. Reverse heat leakage tests were performed in a climate-controlled chamber to determine the overall cabinet thermal conductance (UA). A hot

cycle calorimeter was used to collect the performance data of the compressor. Furthermore, nitrogen flow tests were performed to determine the diameters of the capillary tubes considering the nominal length. Table 1 summarizes most of the refrigerator performance data.

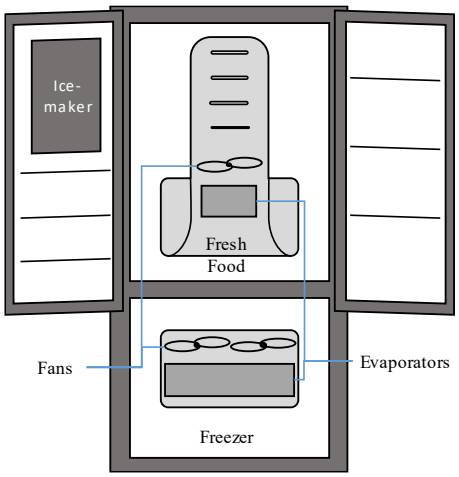

Figure 2. Schematic of the baseline reference refrigerator for this study

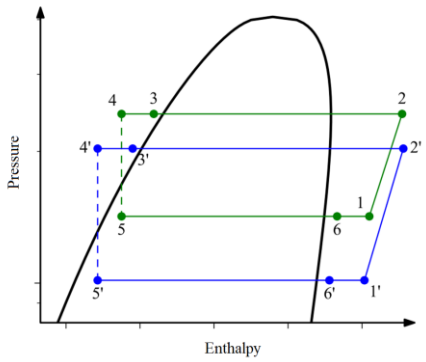

Figure 3. Representation of a parallel dual-evaporator refrigeration loop in a pressure-enthalpy diagram.

In addition, the original refrigerator control logic contained manufacturer heuristics that could not be replicated in the mathematical models. Therefore, a third-party control board was developed and built in-house, making possible to employ a simplified control logic to the refrigerator in question. The developed control board was capable of setting the compressor speed, the 3-way valve position and both the freezer and fresh-food fan speeds by means of a LabVIEW VI interface. Baseline tests using the new control board/logic were performed in a climate-controlled chamber.

Table 1. Experimental data of the FDBM refrigerator components.

Description	**Symbol**	**Value* [unit]**
Condenser heat conductance	UA_c	10.6 - 13.9 [W/K]
Condenser air flow rate	$\dot{V}_c$	14.1 - 38.3 [m³/h]
Fresh-food evaporator heat conductance	$UA_{e,ff}$	17.3- 17.5 [W/K]
Fresh-food evaporator air flow rate	$\dot{V}_{ff}$	13.5 - 28.5 [m³/h]
Freezer evaporator heat conductance	$UA_{e,fz}$	19.2 - 42.8- [W/K]
Freezer evaporator air flow rate	$\dot{V}_{e,fz}$	18.4 - 19.2 [m³/h]
Fresh food to surroundings heat conductance	UA_{ff}	1.941 [W/K]
Freezer to surroundings heat conductance	UA_{fz}	0.832 [W/K]
Ice maker to surroundings heat conductance	UA_{im}	0.071 [W/K]
Fresh food to freezer heat conductance	UA_{ff-fz}	0.285 [W/K]
Fresh food to Icemaker heat conductance	UA_{ff-im}	0.290 [W/K]
Ice maker air flow rate	$\dot{V}_{im}$	2.7- 6.7 [m³/h]

*Upper and lower values are given for minimum and maximum fan speed

3. MATHEMATICAL MODELS

3.1 Condenser

The heat exchanger model adopted for the condenser followed an upwind finite volume scheme as proposed by Laughmann and Qiao (2017). Considering a horizontal straight tube with constant cross-sectional area divided into n control volumes (CVs), one-dimensional flow at axial direction, no pressure drop and homogeneous flow, the mass and energy conservation equations can be expressed as follows:

$$V_j \frac{d\rho_j}{dt} = \dot{m}_k - \dot{m}_{k+1} \tag{1}$$

$$V_j \left[\left(h_j + \frac{\partial h}{\partial \rho}\bigg|_p \right) \frac{d\rho_j}{dt} + \left(\rho_j \frac{\partial h}{\partial p}\bigg|_\rho - 1 \right) \frac{dp}{dt} \right] = (\dot{m}h)_k - (\dot{m}h)_{k+1} + \dot{Q}_j \tag{2}$$

where j stands for the CV average properties and k the CV interfaces, V represents the volume, $\dot{m}$ the mass flow rate, p the pressure, ρ the density, h the specific enthalpy, $\dot{Q}$ the heat transfer rate and t the time. The heat transfer rate is calculated by means of heat transfer coefficient ($\hbar$) correlations such as proposed by Gnielinski (1975) for single-phase flow and Jung *et al.* (2003) for condensing flow.

In addition to the refrigerant side, a set of transient models for the heat exchanger walls were employed. Considering lumped capacity for each control volume, the wall temperature evolution can be described by the following equation:

$$C_w \frac{dT_w}{dt} = \dot{Q}_j - \dot{Q}_{a,j} \tag{3}$$

where C_w is heat exchanger mass thermal capacitance and $\dot{Q}_a$ stands for the air-side heat transfer rate which is determined by means of uniform temperature ε-NTU relationship, *i.e.*, $\varepsilon = 1 - e^{-NTU}$.

3.2 Evaporator

For the evaporator, instead of the finite volume approach, a moving boundaries model was implemented, aiming at reduced computational effort due to a reduced equation set. The derived models were based in the contributions of Wedekind and Stoecker (1968), Gräber *et al.* (2010) and Bonilla *et al.* (2015), where the last two have made contributions specific to the Modelica language.

In summary, the implemented moving boundaries model assumes two nodes, *i.e.*, the phase-changing node and a superheated node, where the flow enters the phase-changing node crosses to the superheated node and then exits the evaporator. Therefore, the evaporator model may assume three states: fully superheated, fully two-phase, or two-phase and superheated. Each state has a triggering condition, *e.g.*, if the two-phase zone length (boundary position) gets below 1 mm then the superheated state is active, whereas if the boundary position get above the total tube length (L) minus 1 mm then the fully two-phase state is active. For the two-phase

Additionally, for the heat exchanger walls, the same approach used for the condenser was considered. For the internal flow (refrigerant side), evaporative heat transfer coefficient correlation by Kandlikar (1990) was employed, whilst for the air side, the appropriate ε-NTU relationships were used alongside the experimental values for air flow rate and overall heat conductance.

In summary, the conservation of mass (global) and conservation of energy equations for the two- and single-phase zones are, respectively

$$\left[L\frac{\partial \rho_v}{\partial p} + \frac{\partial \lambda}{\partial p}(\rho_\ell - \rho_v)(1-\bar{\alpha})\right]\frac{dp}{dt} + (\rho_\ell - \rho_v)\left[(1-\bar{\alpha})\frac{d\lambda}{dt} - \lambda\frac{d\bar{\alpha}}{dt}\right] + G_{\text{out}} - G_{\text{in}} = 0$$

$$\lambda\left\{\left[\rho_v\frac{\partial h_v}{\partial p}\bar{\alpha} + \left(\rho_\ell\frac{\partial h_\ell}{\partial p} - h_{\ell v}\frac{\partial \rho_\ell}{\partial p}\right)(1-\bar{\alpha}) - 1\right]\frac{dp}{dt} - \frac{q''P}{A_C}\right\} + G_{\text{in}}(h_v - h_{\text{in}}) - \rho_\ell h_{\ell v}\left[(1-\bar{\alpha})\frac{d\lambda}{dt} - \lambda\frac{d\bar{\alpha}}{dt}\right] = 0$$

$$G_{\text{out}}(h_{\text{out}} - h_v) - (L-\lambda)\left\{\left[1 - \rho_v\frac{\partial h_v}{\partial p}\right]\frac{dp}{dt} + \frac{q''P}{A_c}\right\} = 0$$

where λ is the two-phase zone length, L is the total length of the heat exchanger, G is the mass flux, $\bar{\alpha}$ is the mean void fraction, P is the perimeter, and A_c is the cross-sectional area. The indices 'in' refer to inlet, 'out' to outlet, ℓ to saturated liquid, and v to saturated vapor.

3.3 Compressor

The compressor model is subdivided into two sub models, namely the compression chamber and the compressor shell. The compression chamber determines the mass flow rate whereas the compressor shell represents an additional volume after the evaporator and impacts significantly on the equalized pressure during the compressor off time. During pull-down or cycling operation, the refrigerator conditions (*e.g.*, working pressures) span a wide range including thermodynamic states far outside the compressor catalogue data. Therefore, the adopted compressor model shall be able to extrapolate the fitting range without significant accuracy compromise.

To this end, Santos *et al.* (2019) proposed a semi-empirical model that was validated for variable- and single-speed compressors as well as for variable-displacement linear compressors, which is the compressor employed in the baseline refrigerator. The proposed model is comprised, essentially, of two equations (one for the mass flow rate and another for the power consumption) with three fitting coefficients each. However, since the compressor operates with variable displacement, the final model is represented by the following expressions:

$$\dot{m}_{\text{max}} = \frac{p_s N}{T_s}\{b_0 - b_1[(p_d/p_s)^{b_2} - 1]\} \tag{4}$$

$$\dot{m}_{\text{var}} = \frac{\dot{W}_{sig}}{a_0 T_s[(p_d/p_s)^{a_1} - 1] + a_2} \tag{5}$$

$$\dot{W} = \frac{\dot{W}_{sig}\dot{m}}{\dot{m}_{\text{max}}} \tag{6}$$

where $\dot{m} = \min(\dot{m}_{\text{max}}, \dot{m}_{\text{var}})$. The fitting coefficients are represented by a and b, the s index represents the compressor suction whereas d is the discharge, 'max' represents the maximum displacement mass flowrate, 'var' the variable-displacement mass flow rate, and 'sig' is the power signal which defines the desired mass flow. It is noteworthy that the a_2 coefficient represents the heat transfer between compressor shell and the surroundings, and therefore should be discounted accordingly when calculating the discharge enthalpy.

3.4 Expansion device

Two capillary tubes are used as expansion devices in the present work. Despite the capillary tube simplicity, the process which undergoes the refrigerant flowing through the tube is rather complex. Several mathematical models have been advanced over decades for the simulation of capillary tubes, most of them report convergence issues and/or slow computation time, *e.g.*, Mezavilla (1995), Hermes (2000) and Mejías (2010). Currently, however, Artificial Neural Networks (ANNs) have gained strength and are being used as mathematical representations for problems across the board. Heimel *et al.* (2014) presented an approach that uses a physical model of the capillary tube (*e.g.*, Hermes *et al.*, 2008), to train an ANN and then later use the ANN itself on the dynamic simulation of the refrigeration system. Such an approach eliminates the mains issues associated with the physical models (convergence and CPU struggle) while maintaining the desired level of physical representation of the capillary tube behavior.

For this work, the model presented by Hermes *et al.* (2008) was implemented in python language and validated against the same data base provided by the authors. With the physical model, a 30,000-point database was adopted for training the ANN. The current guideline for ANN design is not well established and therefore the ANN structure is made empirically through the python library Keras (Chollet *et al.*, 2015). Nonetheless, after training the ANN was validated against the very same experimental dataset used for the first-principles model validation exercise. In addition, some key trendlines of the physical model and the ANN were compared in order to evaluate if the ANN presents in fact a physical representation of the capillary tube behavior (Santos, 2020).

3.5 Check valve

The baseline refrigerator uses a check valve placed at the freezer evaporator outlet to enable fresh-food operation with evaporation temperatures higher than the freezer compartment temperature. Without the check valve and at high evaporation temperatures, the freezer evaporator would become a condenser, trapping refrigerant charge, and thus lowering the evaporation temperature towards the freezer compartment temperature. After freezer operation, however, some liquid refrigerant remains in the freezer evaporator and must be pumped out. This is done by holding the 3-way valve closed and the compressor on during a certain while right before fresh-food operation.

An ideal check valve opens fully when there is positive pressure difference between its inlet and outlet, and is fully closed otherwise. If simulated as such, the check valve model introduces instability to the system model, oscillating rapidly between open and closed state forcing the numerical solver to unacceptably small timesteps. Furthermore, the valve pressure drop cannot be neglected, otherwise the mass flow rate through the valve is undetermined. Therefore, the orifice equation was employed, considering that the orifice area is proportional to the pressure difference, thus making a smooth opening:

$$\dot{m} = C_D A_c \sqrt{\rho_i (p_i - p_o)} \tag{9}$$

$$A_c = \min\left(0, \max\left(A_{\text{max}}\left(\frac{p_i - p_o}{\Delta p_{\text{max}}}\right), A_{\text{max}}\right)\right) \tag{10}$$

where C_D is the discharge coefficient, A_c is the orifice area, A_{max} is the maximum orifice area, Δp_{max} is the maximum pressure difference (where $A_c = A_{\text{max}}$), and the indices 'i' and 'o' refer to inlet and outlet, respectively. In practice, the check valve installed in the refrigerator is a passive (non-spring loaded) check valve, which behaves in a rather non-deterministic manner, therefore the simplified model described above was adopted.

3.6 Refrigerated comparment

The refrigerated compartments have the highest thermal inertia of the refrigerator, orders of magnitude higher than those observed for the refrigeration loop, in such a way that the fully transient model is comprised of a stiff equation set. In order to capture this inertia properly, the polyurethane insulation thermal mass inside the cabinet walls must be

accounted for. This work uses the same approach as reported by Hermes and Melo (2008), employing a one-dimensional heat conduction model and neglecting both convective resistances at the outside and inside surfaces. All imperfections of the insulation are included in an effective thermal conductivity, determined using the experimental overall heat conductance (UA).

The following equations summarizes the model, the first being a central control volume of the discrete wall, and the second the lumped refrigerated space:

$$(\rho c)_w \frac{dT_{k,w}}{dt} = \frac{k_w}{\Delta z^2}\left(T_{k+1,w} + T_{k-1,w} - 2T_{k,w}\right)$$

$$\left(C_{\text{lin}} + \frac{\rho V c_p T_{\text{amb}}}{T}\right)\frac{dT}{dt} = \frac{k_w A}{\Delta z/2}\left(T_{N,w} - T\right) + \rho\dot{V}(T_i - T) + \sum\dot{Q}$$

where T denotes the temperature, Δz is the wall control volume size ($\Delta z = L_w/N$), k is the equivalent thermal conductivity, C_{lin} is the plastic liner thermal capacity, V is the compartment internal volume, $\dot{V}$ is the air flow rate, and $\sum\dot{Q}$ is the heat transfer between compartments. The indices w refer to the wall, 'amb' to the surrounding ambient, and i the insufflation point.

3.7 Refrigeration system solution (fully transient and quasi-steady)

The fully transient solution of the refrigeration system is simply the coupling of all component sub models, where the mass flow rate at control volumes inlet and outlet transports the refrigerant enthalpy across all components. However, it is necessary to establish the proper initial conditions of the problem state variables, *i.e.*, the working pressures, enthalpies, densities, and temperatures. During initialization, it is assumed that the system is in equilibrium with the surrounding environment, therefore all temperatures are equal to T_{amb}. Furthermore, condensing and evaporating pressures are also in equilibrium and the refrigerant charge is spread uniformly in the refrigeration loop, therefore the initial density is $\rho = M/\sum V_j$, where M is the refrigerant charge (135 g of HFC-134a) and j denotes each of the refrigeration system components – the initial enthalpy of the refrigerant is computed by means of property functions.

The quasi-steady-state approach, however, requires further simplifications. The key assumptions in this case are prescribing superheating and subcooling degrees at the evaporator and condenser outlet, respectively. By doing so, it is possible to neglect the refrigerant charge inventory and tube model entirely, thus meaning that the refrigerant-side equations are reduced to properties computations only, which significantly reduces the number of equations and problem complexity. In fact, the fully transient model was comprised of about 1100 equations whilst the quasi-steady-state required 197 equations only.

4. RESULTS AND DISCUSSIONS

Figures 4 and 5 show simulations results for the fully transient and quasi-steady-state modeling strategies, respectively. On both figures, the left side shows the pull-down whereas the right side shows the cycling regime. At first, it can be noticed that the fully transient method has captured the pull-down regime reasonably well, whilst the quasi-steady-state model has failed in this regard. Such an outcome can be understood given that the key assumption of the quasi-steady-state approach is that both evaporators and condenser are full at all instants. This overestimates the cooling capacity, particularly during the refrigerator pull-down, where the mass migration effects take more importance.

Furthermore, a pressure peak is observed at the experimental data (at about 1 hour), however the peak is flattened in the simulation result. This outcome is related to the homogenous two-phase flow models adopted in the condenser and could be addressed by implementing a void fraction model. The differences in the evaporating pressure may be related to the chosen void fraction model as well – the present work used the void fraction proposed by Cioncolini and Thome (2012), however others could be explored. A simulated Design of Experiments (DoE), such as performed by Hermes (2006), could help to choose more suitable void fraction models. Observing the quasi-steady-state model, however, one can note that the pressure peak is not captured, again due to the assumption of prescribed superheating and subcooling degrees.

On the other hand, during the cycling regime the quasi-steady-state model performs well, making fair predictions for the compartment temperatures, working pressures and, consequently, power consumption. Both the fully transient and quasi-steady-state simulation models yielded reasonably accurate results for the cycling regime: the energy consumption deviation of the latter was -7.7%, and -3.0% for the former, yet the CPU time of the two strategies were significantly apart.

The fully transient simulation model was able to compute about 2 min of operation per second of CPU, whereas the quasi-steady-state could do nearly 6 times that much: 13 min/s_{CPU}. In addition, the latter also outperformed the former when it came to robustness. The fully transient model presented several convergence issues and required attention to

details such as the smoothing of sharp transitions, or division by zero. Such issues were not encountered while working with the quasi-steady-state simulation model.

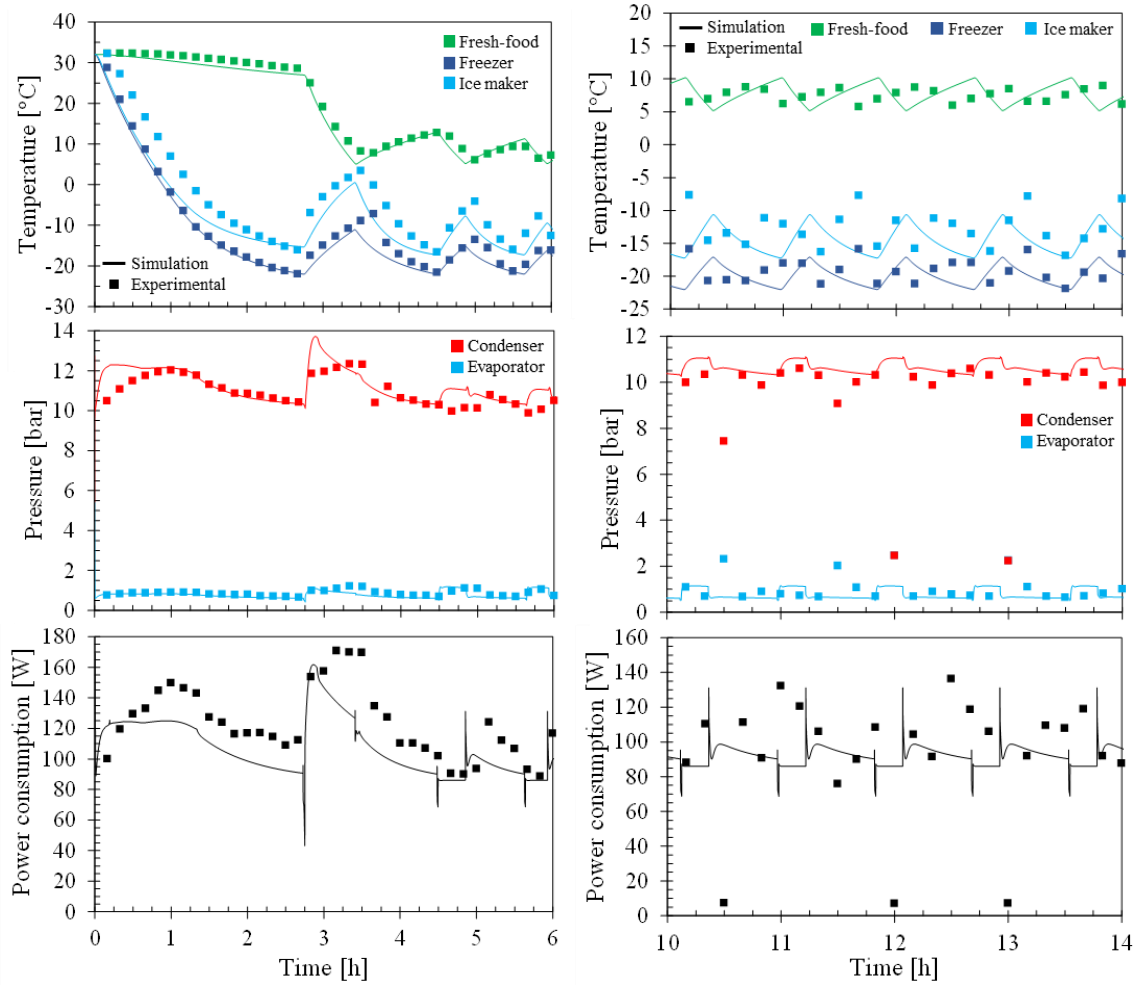

Figure 4. Fully transient simulation vs. experimental data for a pull down (left) and cycling regime (right). Conditions as laid out in Table 2

Additionally, both simulation models were used to assess the model capability of predicting the system performance after changes in the refrigerator control logics. For instance, the pump out time was changed, in the experiment, from 30 s to 0 s and as a result the energy consumption dropped from 69.1 kWh/month to 66.1 kWh/month (-4.3%). Doing the same change in the fully transient model, the energy consumption dropped from 67.0 kWh/month to 66.2 kWh/month (-1.2%). Since the quasi-steady-state model neglects the refrigerant side entirely, the pump out time cannot be assessed.

On the other hand, other aspects of the control logic may be explored as well as its impacts on the refrigerator energy consumption. In this case, a new control logic was proposed, where the freezer compartment holds priority over the fresh-food compartment, *i.e.*, if the freezer temperature rises above the thermostat maximum, the 3-way valve is directed to freezer operation regardless of the fresh-food temperature. By applying this new control logic to the experimental setup, the refrigerator energy consumption increased from 64.7 kWh/month to 66.8 kWh/month (+3.2%). Doing the same on the fully transient model, the energy consumption increased from to 59.7 kWh/month to 61.7 kWh/month (+3.3%), the very same variation observed experimentally.

5. FINAL REMARKS

The present paper has presented simulation results of a combi refrigerator by means of two modeling strategies, namely fully transient and quasi-steady-state. It was possible to conclude that both strategies can represent reasonably well the refrigeration system. However, the quasi-steady-state simulation model capabilities are limited to the cycling regime, whereas the fully transient extend also to the pull-down operation. Nonetheless, the quasi-steady-state model was far more efficient, being able to simulate nearly 6 times faster than the fully transient model, without any convergence or numerical issues that were present in the fully transient simulation model. Additionally, since both

strategies are capable to simulate the cabinet dynamics, they can be used to assess different control logics and their impact upon the refrigerator performance. However, depending on the chosen model, some control features may not be available and, therefore, cannot be assessed, such as the pump out time in the case the quasi-steady-state model is used.

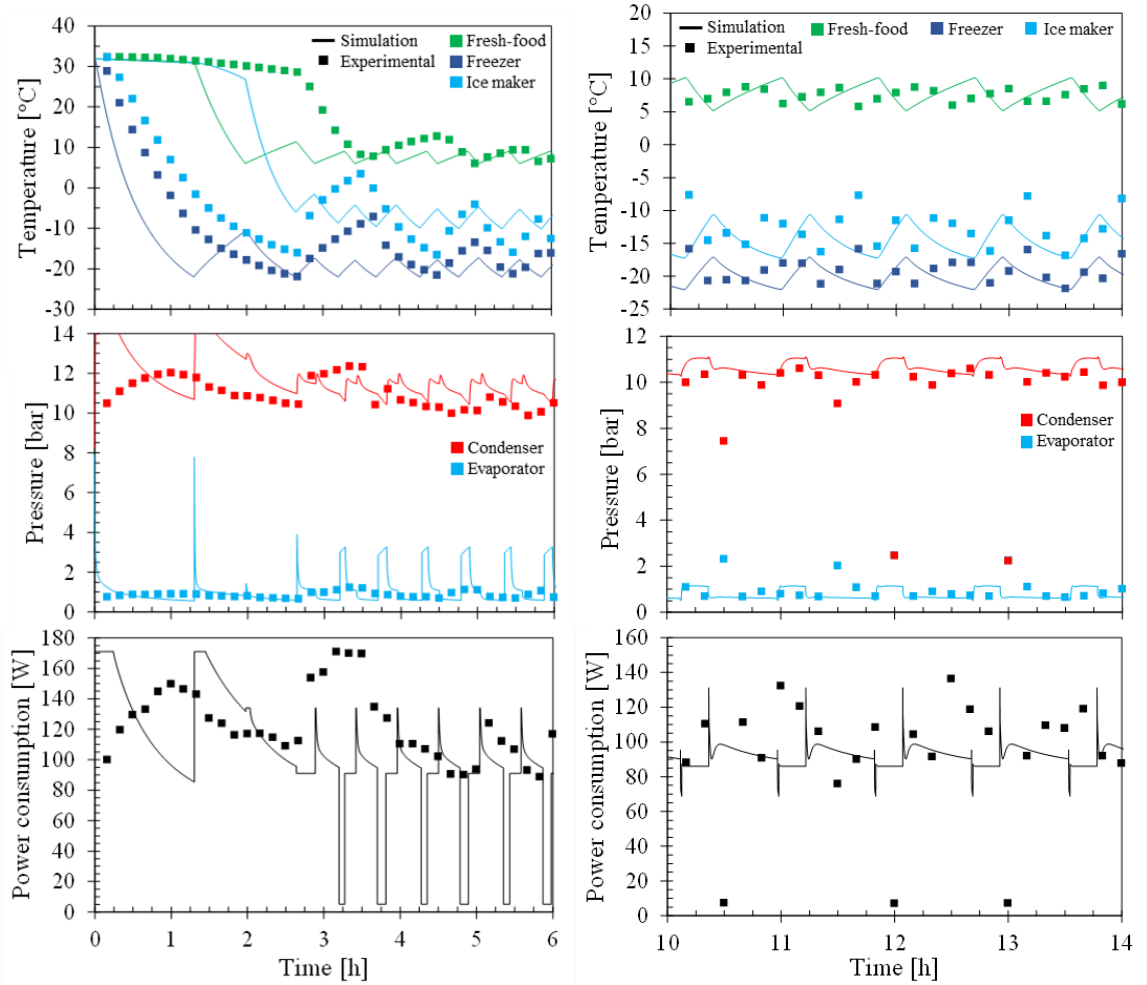

Figure 5. Quasi-steady-state simulation vs. experimental data for a pull down (left) and cycling regime (right). Conditions as laid out in Table 2

6. ACKNOWLEDGEMENTS

The authors appreciate the support from Whirlpool, Embraco and EMBRAPII. Additional funding was provided by the National Institutes of Science and Technology (INCT) Program (CNPq Grant Nº. 404023/2019-3; FAPESC Grant Nº. 2019TR0846).

7. REFERENCES

Bonilla, J., Dormido, S. and Cellier, F.E., 2015. “Switching moving boundary models for two-phase flow evaporators and condensers”. Comun Nonlinear Sci Numer Simulat, Vol. 20, pp. 743–768.

Borges, B.N., Hermes, C.J.L., Gonçalves, J.M. and Melo, C., 2011. “Transient simulation of household refrigerators”. Applied Energy, Vol. 88, pp. 748–754.

Borges, B.N., 2013. Modelagem semi-empírica de um refrigerador frost-free sujeito à abertura de portas. Mestrado em engenharia mecânica (dissertação), Universidade Federal de Santa Catarina.

Butrymowicz, D., mierciew, K., Karwacki, J. and Gagan, J., 2014. “Experimental investigations of low-temperature driven ejection refrigeration cycle operating with isobutane”. Int J. Refrig, Vol. 39, pp. 196–209.

Cioncolini, A. and Thome, J. R., 2012. “Void fraction prediction in annular two-phase flow”. International Journal of Multiphase flow, n. 43, p. 72–84.

Chollet, F. *et al.*, 2015. “Keras”. https://keras.io.

Diniz, M.C., Hermes, C.J.L. and Deschamps, C.J., 2019. “Transient simulation of small-capacity reciprocating compressors in on-off controlled refrigerators”. Int J. Refrig, Vol. 102, pp. 12–21.

Eletrobrás and Procel, 2005. “Pesquisa de posse de equipamentos e hábitos de uso”.

Gnielinski, V., 1976. “New equations for heat and mass transfer in turbulent pipe and channel flow”. International Chemical Engineering, Vol. 16, No. 2, pp. 359–367.

Gräber, M., Strupp, N.C. and Tegethoff, W., 2010. “Moving boundary heat exchanger model and validation procedure”. In EUROSIM Congress of Modelling and Simulation.

Heimel, M., Lang, W. and Almbauer, R., 2014. “Performance prediction using artifical neural network for isobutane flow in non-adiabatic capillary tubes”. Int J. Refrig, Vol. 38, pp. 281–289.

Hermes, C.J.L., 2000. Desenvolvimento de modelos matemáticos para a simulação numérica de refrigeradores domésticos em regime transiente. Mestrado em engenharia mecânica (dissertação), Universidade Federal de Santa Catarina.

Hermes, C.J.L., 2006. Uma metodologia para simulação transiente de refrigeradores domésticos. Doutorado em engenharia mecânica (tese), Universidade Federal de Santa Catarina, Florianópolis, SC, BR.

Hermes, C.J.L., Knabben, F.T., Melo, C. and Gonçalves, J.M., 2009. “Prediction of the energy consumption of household refrigerators and freezers via steady-state simulation”. Applied Energy, Vol. 86, pp. 1311–1319.

Hermes, C.J.L., Melo, C. and Gonçalves, J.M., 2008. “Modeling of non-adiabatic capillary tube flows: A simplified approach and comprehensive experimental validation”. Int J. Refrig, Vol. 31, pp. 1358–1367.

INMETRO, 2021. “Tabelas de consumo/eficiência energética”. URL http://www.inmetro.gov.br/consumidor/tabelas.asp. Last access: 2021-09-14.

Jakobsen, A., 1995. Energy optimisation of refrigeration systems. Ph.d. thesis, Technical University of Denmark.

Jung, D., Song, K.H., Cho, Y. and Kim, S.J., 2003. “Flow condensation heat transfer coefficients of pure refrigerant”. Int J. Refrig, Vol. 26, pp. 4–11.

Kandlikar, S.G., 1990. “A general correlation for saturated two-phase flow boiling heat transfer inside horizontal and vertical tubes”. ASME Journal of Heat Transfer, Vol. 112, pp. 219–228.

Klein, S.A., 2011. “Engineering equation solver”.

Knabben, F.T., 2019. Aplicabilidade de dispositivos de expansão variável em refrigeradores domésticos. Doutorado em engenharia mecânica (tese), Universidade Federal de Santa Catarina.

Laughman, C.R. and Qiao, H., 2017. “On the influence of state selection on mass conservation in dynamic vapour compression cycle models”. Mathematical and Computer Modelling of Dynamical Systems, Vol. 23, No. 3, pp. 262– 283.

Mejías, N.A., 2010. Numerical Simulation and Experimental Validation of Vapor Compression Refrigerating Systems. Special Emphasis on Natural Refrigerants. Doctoral thesis, Universidad Politécnica de Catalunya.

Mezavilla, M.M., 1995. Simulação do escoamento de fluidos refrigerantes em tubos capilares não-adiabáticos. Mestrado em engenharia mecânica (dissertação), Universidade Federal de Santa Catarina.

Modelica Association, 2020. “Modelica”. URL www.modelica.org.

Negrão, C.O.R. and Hermes, C.J.L., 2011. “Energy and cost savings in household refrigerating appliances”. Applied Energy, Vol. 88, No. 9, pp. 3051–3060.

Radermacher, R. and Kim, K., 1996. “Domestic refrigerators”. Int J. Refrig, Vol. 19, No. 1, pp. 61–69.

Santos, G.Z. dos, Ronzoni, A.F. and Hermes, C.J.L., 2019. “Performance characterization of small variable-capacity reciprocating compressors using a minimal dataset”. Int J. Refrig, Vol. 107, pp. 191–201.

Santos, G.Z. dos, 2020. Uma análise comparativa entre estratégias para a simulação transiente de refrigerdores domésticos com dois evaporadores em paralelo. Mestrado em engenharia mecânica (dissertação), Universidade Federal de Santa Catarina.

Shah, R., Alleyne, A.G., Bullard C.W., Rasmussen, B.P., and Hrnjak P.S., 2003. Dynamic modeling and control of single and multi-evaporator subcritical vapor compression systems. Urbana, IL, USA.

Wedekind, G.L. and Stoecker, W.F., 1968. “Theoretical model for predicting the transient response of the mixture-vapor transition point in horizontal evaporating flow”. Journal of Heat Transfer, pp. 165–174.

8. RESPONSIBILITY NOTICE

The authors are the only responsible for the printed material included in this paper.